MoS_2 Functionalized Multicore Fiber Probes for Selective Detection of *Shigella* Bacteria Based on Localized Plasmon

Santosh Kumar, *Senior Member, OSA/IEEE*, Zhu Guo, Ragini Singh, Qinglin Wang, Bingyuan Zhang, Shuang Cheng, Feng-Zhen Liu, Carlos Marques, Brajesh Kumar Kaushik, *Senior Member, IEEE*, and Rajan Jha, *Senior Member, OSA*

***Abstract*—Present study demonstrates the fiber-optic localized surface plasmon resonance (LSPR) based sensitive biosensor for detection of *Shigella* bacterial species. The proposed sensor is comprised of multi-core fiber (MCF) having seven cores arranged in a hexagonal shape and spliced with single-mode fiber (SMF) for efficient detection. An increase in evanescent waves (EWs) and coupling of modes between MCF cores was achieved by etching process in a controlled manner. The etching process also increases the refractive index sensitivity (RIS) of the proposed sensor. Further, coating with nanomaterials like gold nanoparticles (AuNPs) and molybdenum disulfide (MoS_2) helps in the excitation of localized plasmons. Here, *Shigella* specific oligonucleotide probes are used as a recognition element. The results demonstrate that the proposed sensor can successfully and efficiently detect the *Shigella* bacterial species with high sensitivity. *Shigella* in the range of 10 – 100 CFU/mL (colony-forming unit/mL) can cause serious intestinal infection and therefore, its detection in this range is critical. The proposed sensor demonstrates a linearity range from 1 to 10^9 CFU/mL with a detection time of 5 min and a limit of detection (LoD) of 1.56 CFU/mL. The proposed sensing methodology can be a potential alternative to the commercially existing ones in the near future.**

***Index Terms*—Gold nanoparticles (AuNPs), localized surface plasmon resonance, molybdenum disulfide (MoS_2), multicore fiber, optical fiber biosensor, *Shigella*.**

Manuscript received September 16, 2020; revised October 25, 2020 and November 4, 2020; accepted November 5, 2020. Date of publication November 9, 2020; date of current version June 16, 2021. This work was supported in part by the Double-Hundred Talent Plan of Shandong Province; in part by the National Key Research & Development Program of China under Grant 2016YFB0402105, in part by the Belt and Road Special Project approved by Shandong Province for Introduction of Foreign Experts in 2018, in part by the Liaocheng University of China under Grant 318051901, Grant 31805180301, and Grant 31805180326; in part by the Science and Technology Plan of Youth Innovation Team for Universities of Shandong Province under Grant 2019KJJ019; in part by the Introduction and Cultivation Plan of Youth Innovation Talents for Universities of Shandong Province; and in part by the Science and Engineering Research Board, India under Grant TAR/2018/000051. The work of C. Marques was supported in part by the Fundação para a Ciência e a Tecnologia (FCT) through the CEECIND/00034/2018 (iFish Project), UIDB/50025/2020, and UIDP/50025/2020 i3N projects; and in part by the National Funds through FCT/MEC. *(Corresponding author: Santosh Kumar.)*

Santosh Kumar, Zhu Guo, Qinglin Wang, and Bingyuan Zhang are with the Shandong Key Laboratory of Optical Communication Science and Technology, School of Physics Science and Information Technology, Liaocheng University, Liaocheng 252059, China (e-mail: santosh@lcu.edu.cn; 2902831435@QQ.com; wangqinglin@lcu.edu.cn; zhangbingyuan@lcu.edu.cn).

Ragini Singh and Shuang Cheng are with the School of Agronomy, Liaocheng University, Liaocheng 252059, China (e-mail: singh@lcu.edu.cn; chengshuang@lcu.edu.cn).

Feng-Zhen Liu is with the Liaocheng People's Hospital, Medical College of Liaocheng University, Liaocheng 252000, China (e-mail: ldcllfz@163.com).

Carlos Marques is with the I3N & Physics Department, University of Aveiro, 3810-193 Aveiro, Portugal (e-mail: carlos.marques@ua.pt).

Brajesh Kumar Kaushik is with the Department of Electronics and Communication Engineering, Indian Institute of Technology Roorkee, Roorkee 247667, India (e-mail: bkk23fec@iitr.ac.in).

Rajan Jha is with the Nanophotonics and Plasmonics Laboratory, School of Basic Sciences, Indian Institute of Technology Bhubaneswar, Bhubaneswar 751013, India (e-mail: rjha@iitbbs.ac.in).

Color versions of one or more of the figures in this article are available online at https://ieeexplore.ieee.org.

Digital Object Identifier 10.1109/JLT.2020.3036610

I. Introduction

Shigella is an enteric bacterial species that infects humans and develops symptoms like cramping, fever, diarrhea, vomiting, and other serious complications. World health organization (WHO) reported that worldwide *Shigella* case is around 164.7 million with 1.1 million death, mostly children under a 5-year age group whereas in adults, a 10-100 colony-forming unit (CFU) of *Shigella* causes intestinal infection with serious inflammation [1]. Several developing countries suffer due to lack of clean water supply, poor sanitation, malnutrition, and overcrowding, which induces high dysentery cases.

Various traditional methods like a serological test, bacterial cultivation, and polymerase chain reaction (PCR) are available for detection of different bacterial species [1]–[5]. However, conventional methods suffer from several limitations like time-consuming, labour intensive, low sensitivity and specificity, complex procedure, and costly equipment, which prevent their application for easy real-time detection of samples. Thus, it is of great importance to develop a fast and effective method for detection of bacteria like *Shigella*. Reports are available demonstrating about fiber optic-based biosensor for detection of various bacterial species [1], [6], [7]. Xiao et al. [1] demonstrated the *Shigella* detection with the help of fluorescence tagged complementary oligonucleotide. The result showed that fully complementary oligonucleotide exhibits high fluorescence signal in comparison of non-complementary or partial complementary probe, which prove that the signal is generated due to hybridization of probe and not from non-specific adsorption which proves the efficacy of sensor.

On the other hand, plasmonic sensors have shown great promise in the last few decades [8], [9]. Integrating the plasmonics concept with optical fiber especially, the absorption-based fiber-optic localized surface plasmon -resonance (LSPR) sensors are promising as it is easier to fabricate and demonstrate a real-time response, economical, disposable, and simple to implement [10]–[13]. LSPR is the density oscillations of conduction electrons inside metallic nanoparticles under the influence of incident electromagnetic radiation. Advancement in nanotechnology field leads to its broad application in biosensing including detection of bacterial cells from real samples. Various nanoparticles like gold nanoparticles (AuNPs), and molybdenum disulfide (MoS_2) have been frequently used for the biosensing application [14]. On the other hand, MoS_2 has unique properties like thermal stability, low toxicity, high surface to volume ratio, high electron mobility, presence of free sulfur group for hydrophobic interaction that has drawn the interest of scientific community for application in biosensing [15] and lower full width at half maximum [16]. In this regard, Kaushik *et al.* developed the MoS_2 nanosheet functionalized fiber-optic SPR biosensor for sensitive detection of *E.coli* [14]. Immunosensor was developed by immobilizing the *E.coli* monoclonal antibodies and using wavelength interrogation method, exhibiting a strong linear relationship with increasing concentration of *E.coli*. It is nonspecific to other bacteria groups and exhibits practical application in a real sample like water and orange juice. Further, Halkare *et al.* also developed the AuNPs based LSPR biosensor for detection of *E.coli* using bacteriophage as a recognition element [17]. As the bacteriophage reacts with specific bacterial strain, the proposed sensor can be employed in detection of a specific bacterial strain only.

This study uses a versatile Multi-Core Fiber (MCF) structure for sensing of *Shigella*. MCF offers many advantages like high sensitivity to small refractive index (RI) variations due to inter-coupling between cores of MCF, compact architecture, low connection loss with Single-Mode Fiber (SMF), and easy fabrication [18]. MCF consists of the multiple cores inside common cladding of optical fiber that offers high degrees of freedom in fiber parameters [19]. MCF, being a versatile wave-guiding system, has been often used for developing sensors for RI [20]–[22], shape [23], vibration [24], [25], twist [26], temperature [18], [27], strain [28], and bending [29], [30].

To our knowledge, this is the first paper that demonstrates the AuNPs and MoS_2-immobilized MCF based processed system for detection of *Shigella* bacteria. Here, the proposed online sensor uses a short segment of MCF spliced with SMF using a fusion splicer in a controlled manner [31]. Thereafter, the MCF surface is immobilized with MoS_2/Au-NPs in a controlled process to develop a miniaturized probe for sensing. Encouragingly, the linearity range of proposed sensor for *Shigella* bacteria is quite high (1 to 10^9 CFU/mL), detection time (5 min) is less and the detection limit (1.56 CFU/mL) is significantly low.

II. Experimental Section

A. Materials and Instruments

Step index single-mode optical fiber (Core diameter: 9 μm, cladding diameter 125 μm) was procured from Shenzhen EB-link Technologies Co., Ltd, China. Multi-core fiber (Core diameter: 6.1 μm, cladding diameter 125 μm) was purchased from Fibercore Ltd., UK. Hydrogen tetrachloroaurate ($HAuCl_4$), tri-sodium citrate, molybdenum disulfide (MoS_2) powder (234842, Sigma-Aldrich), n-methyl pyrrolidone (NMP), 11-Mercaptoundecanoic acid (11-MUA), Acetone, hydrogen peroxide (H_2O_2), sulfuric acid solution (H_2SO_4), ultrapure water, (3-mercaptopropyl) trimethoxysilane (MPTMS), Phosphate-buffered saline (PBS), N-(3-Dimethylaminopropyl)-N'-Ethyl carbodiimide hydrochloride (EDC), and N-Hydroxysuccinimide (NHS) were purchased from Sigma-Aldrich, Shanghai. *Shigella sonnei* (*S. sonnei*) (BNCC 108852) bacteria purchased from BeNa culture collection, China. The sequences of all DNA oligonucleotides (FC-TGT, 190916L87; BPM-TGT, 190916L88; NC-TGT, 190916L89, and IPA Probe, 190916A16) were purchased from Shanghai Generay Biotech Co., Ltd, China. Bovine serum albumin (BSA), streptavidin (SA), and (3-aminopropyl)triethoxysilane (APTES) from Shanghai Aladdin Bio-Chem Technology Co., LTD, China. Nutrients such as peptone, beef powder, sodium chloride (NaCl), and agar were procured from a local vendor, Liaocheng, China. All reagents were of analytical grades and used without further purification in the experiment. De-ionized (DI) water of specific resistivity ($>$18 MΩ.cm) obtained from Milli-Q system was used to prepare all aqueous solutions.

The optical characteristics of AuNPs and MoS_2-NPs solutions were analyzed by an Ultraviolet-visible (UV-Vis) spectrophotometer (HITACHI-3310). The MoS_2-NPs synthesis was carried out using an ultrasonic cleaner, sonicator probe (Ningbo Scientz Biotechnology Co., Ltd., China), and centrifugation machine. The morphology of NPs was determined by a high-resolution transmission electron microscope (HR-TEM) (Talos L120C, Thermo Fisher Scientific) and compositional analysis was determined by Energy Dispersive X-ray (EDX) spectroscope attached to TEM. The autoclave was used to prepare the media and clean the glassware. A Shaker incubator was used to grow the bacteria and a biosafety cabinet was used to perform the bacterial experiment. The Field Emission Scanning Electron Microscopy (FE-SEM, Gemini, Carl Zeiss Microscopy) was used to characterize the NP-immobilized sensor probe.

B. Fabrication of Sensor Probe

To fabricate the sensor structure, an advanced fusion splicer (FSM-100 P+ ARC Master, Fujikura) was used to splice the short section of MCF with SMF as shown in Fig. 1 [22], [31], [32]. The core and cladding diameter of SMF is 9 μm and 125 μm, respectively which is close to core (6.1 μm) and cladding diameter (125 μm) of MCF hence facilitates the splicing and the spliced image is shown in Fig. 1. The splicing has been performed using cladding alignment technique and the typical coupling loss is less than 0.01 dB. First, polymer coating of fiber was removed by a stripper, and dust over fiber was cleaned by ethanol before splicing. After splicing, 1 mm of MCF section was considered for the sensor probe, thus sensor structure is named as SMF-MCF probe. The core of MCF is

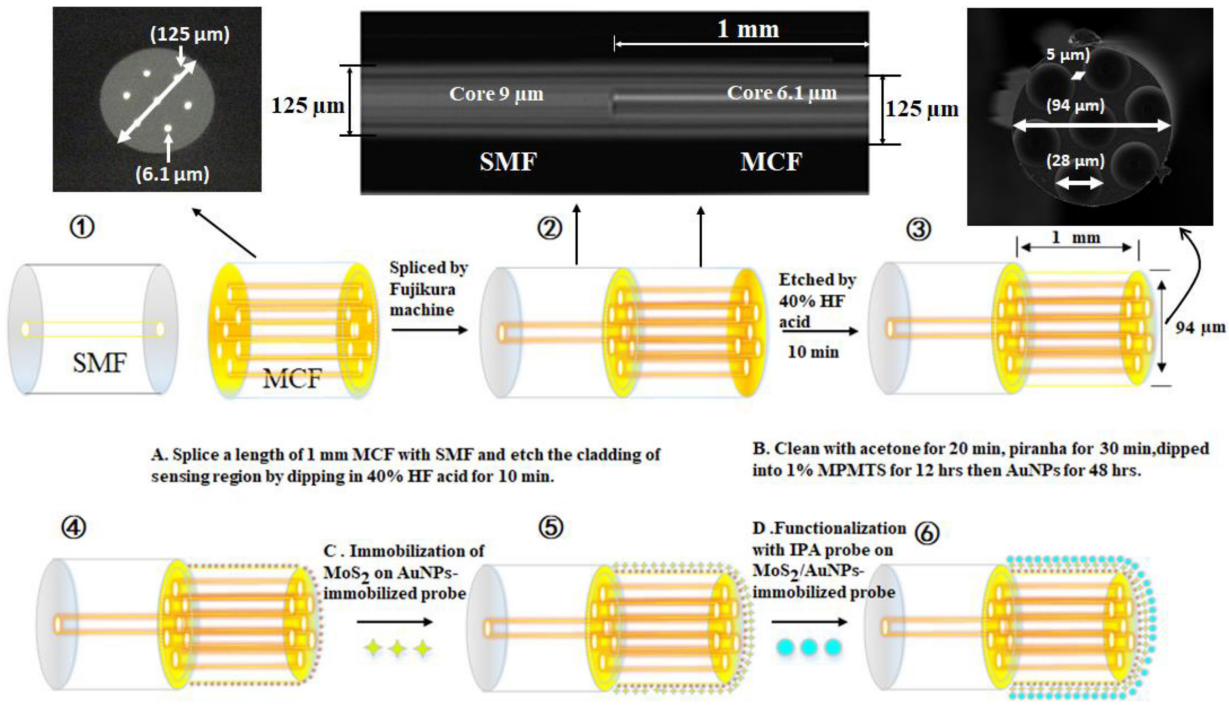

Fig. 1. Fabrication steps of MoS_2/Au-NPs-immobilized SMF-MCF fiber sensor probe.

highly germanium doped as compared to SMF. Thereafter, to emanate the evanescent waves (EWs) and coupling of modes, sensor structure was etched using 40% hydrofluoric acid (HF) for 15 min. Thus, there are two types of sensor structure: namely probe 1: unetched probe and probe 2: etched probe. The sensor was developed using both probes and the sensing performance was compared.

The proposed sensing probes primarily work on core mismatch technique since core diameter of SMF and MCF are 9 μm and 6.1 μm respectively. This helps in excitement of several modes inside the MCF that propagate through its seven cores. A reduced cladding diameter of etched fiber and wide cores help increase the sensitivity of the proposed sensor. Here, wide cores map to expanded mode-field radius of an MCF by etched expanded core (EEC) technique [32]. In EEC, heat is generated at germanium doped core due to HF acid, thus expanding the core of MCF from 6.1 μm to 28 μm in a uniform way (as shown in Fig. 1).

The outer cladding thickness, i.e., the minimum distance between cladding outer surface and center of outermost core, also decreases due to etching. The EWs from outermost core also couples to the coating surface and helps in sensing by interaction with analytes [19]. The protocol for synthesis of AuNPs [33] and MoS_2-NPs [14] are discussed in Section A.I.A of Appendix. Immobilization technique is discussed in detail in Section A.I.B of Appendix using Fig. 1 [34]. The schematic for LSPR measurements is discussed in Section A.I.C of Appendix using Fig. A-1 [35]. The light from the tungsten-halogen source is launched at the 1st end of the bifurcated cable and is coupled to the sensing probes through an adapter connected at the 2nd end of the bifurcated cable. The light interacts with the functionalized probe and the reflected light from the tip of the sensor goes

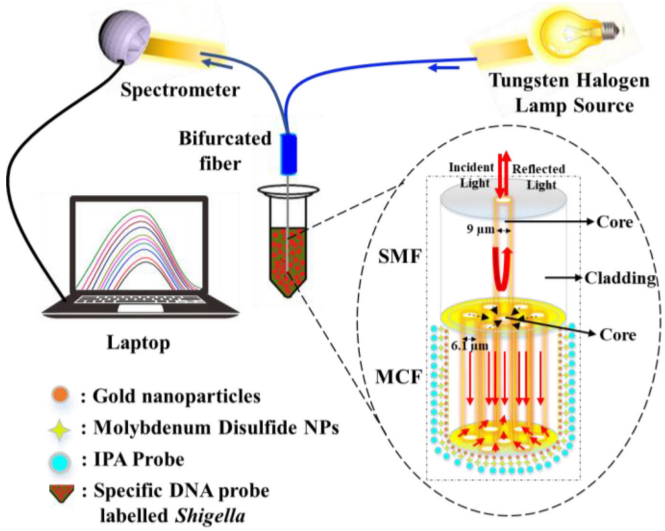

Fig. 2. Experimental setup for detection of *Shigella* bacteria using a proposed sensor probe.

to the spectrometer through the 3rd end of the bifurcated cable as shown in Fig. 2. Culture steps (37 °C for 48 h in aerobic conditions) of *Shigella sonnei* bacteria is discussed in Section A.I.D of Appendix using Fig. A-2.

III. Results and Discussion

A. Characterization of Nanoparticles

The morphology of NPs plays an important role in the fabrication of biosensors, thus require proper characterization to improve sensing performance. The primary investigation of NPs

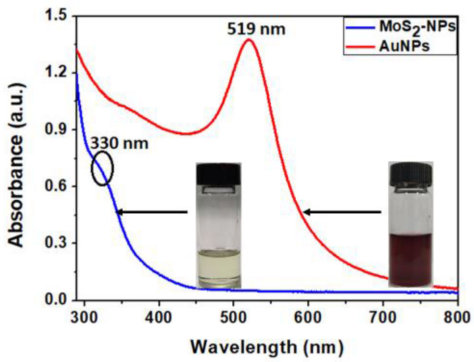

Fig. 3. UV-Vis absorbance spectrum of AuNPs, and MoS_2-NPs solution along with their images.

can be performed by measurement of absorbance spectrum using a UV-Vis spectrophotometer as shown in Fig. 3. The peak absorbance wavelength of synthesized AuNPs and MoS_2-NPs was found at 519 nm and 330 nm, respectively. The morphology and material composition of NPs are shown in Fig. A-3 of Appendix.

HR-TEM image (Fig. A-3a) shows the synthesized AuNPs are spherical, whereas, Fig. A-3b shows the TEM-EDS analysis of the synthesized AuNPs confirming the presence of gold (Au). Similarly, Fig. A-3c shows the HR-TEM image of spherical MoS_2-NPs, and Fig. A-3d is a TEM-EDS image that shows the material composition of synthesized NPs as molybdenum (Mo). The size of the synthesized AuNPs is obtained through ImageJ software that is shown as a histogram in Fig. A-3a (Inset). As the chemical route for synthesis limits the size uniformity, this shows the average diameter of AuNPs as 13 nm. As per earlier experimental data, this size of AuNPs is more sensitive for detection of living organisms [22]. Similarly, average diameter of MoS_2-NPs is found as 2.3 nm as shown in Fig. A-3c (Inset).

B. Characterization of a Nanoparticles-coated Sensor Probe

Characterization of sensor probe was performed by imaging of NPs-immobilized probe through FE-SEM. Fig. 1 shows the cross-sectional view of non-etched- and etched multicore fiber. In non-etched fiber, the core diameter is 6.1 μm that is visible in the CCD image and seven core of diameter 28 μm is observed in etched fiber of Fig. 1. The core of MCF is highly Ge-doped that etch easily in HF-acid and widen the core diameter. The cladding diameter of non-etched and etched fiber is 125 μm and 94 μm, respectively as shown in Fig. 1.

Then, to check the coating of NPs over sensor structure, NPs-immobilized probe was characterized using FE-SEM at lower and higher magnification. Fig. A-4a (Appendix) shows the picture of sensor structure at lower magnification (30 X). The NPs around sensor surface can be also seen at higher magnification. Fig. A-4b shows the coating of AuNPs, whereas Fig. A-4c shows the coating of AuNPs and MoS_2-NPs over fiber structure. The thin coating of 2.3 nm of MoS_2-NPs exists over 13 nm-AuNPs. Fig. A-6a and A-6b show the SEM images of sensor probe before and after detection of *Shigella* bacteria at the same magnification (5 KX), respectively. It can be seen from the figures that there is a regular arrangement of the bacterial cells over the functionalized probe after an interaction. This can be attributed that hybridization takes place at the fiber surface and changes the RI based on the concentration (CFU/mL) of *S. sonnei* [1].

TABLE I
DIFFERENT OLIGONUCLEOTIDES[A] USED FOR SENSING OF *SHIGELLA SONNEI* [1]

Name	Sequence (5' – 3')
IPA Probe[B]	Biotin-TTTTTTTTTTTTAGTCTTTCGCTGTTGCTGCTGATGCC
FC TGT[C]	Cy5.5-GGCATCAGCAGCAACAGCGAAAGACT
BPM TGT[C]	Cy5.5-GGCATCAGCACCAACAGCGAAAGACT
NC TGT[C]	Cy5.5-TGGCAGAGCGGGTACTAACATGATT

[A]TGT – target; FC – fully complementary; BPM – base pair mismatched; NC – non-complementary; [B]Receptor; [C]Analyte.

C. LSPR Sensing Results

The MoS_2/AuNPs-immobilized sensor probe was further incubated in 12 μL of 100% acetic acid, 150 μL of 98% APTES, and 12 mL of 95% ethanol for 30 min at room temperature. The unbounded APTES molecules were removed by ethanol and fiber was dried by N_2 gas. Further, an aminated sensor probe was kept in 10% glutaraldehyde solution for 1 h. Thereafter, it was kept in 0.05 mg/mL SA for 3 h and rinsed with PBST solution (PBS plus 0.05% Tween 20). The SA-immobilized fiber sensing probe was further functionalized with a 1 μM biotin-labeled IPA DNA probe dissolved in TE buffer for 1 h. The TE buffer was prepared using the 20 mM Tris-HCl of pH 8.0 and 0.5 M $MgCl_2$. Then, biotin-labelled probe was rinsed with PBST and kept in a 1% BSA solution for 1 h to block the non-specific absorption sites.

For *S. sonnei* bacterial detection, solutions of different concentrations in the range of 1 to 10^9 CFU/mL were prepared. Further, several oligonucleotide probes were used i.e., Fully Complementary probe (FC) which can exactly bind to the target site and produces high fluorescence and absorbance, One-Base mismatched probe (BPM) which cannot bind firmly to target site and thus produces very low fluorescence and low absorbance, and Non-complementary probe (NC) which cannot bind to target site at all and thus no fluorescence and very low absorbance signal can be produced. Table I shows the sequences of DNA oligonucleotides used for the sensing of *Shigella sonnei*. 200 μL of Cy5.5-labeled probe was dissolved in 1 mL of *Shigella Sonnei* bacterial solution and centrifuged it for 5 min. Thereafter, the pellet was dissolved in PBS and allowed for hybridization with the DNA probe on fiber surface through SELEX process [36]. To measure the different concentrations (CFU/mL) of *Shigella*, the sensor probe was regenerated using 0.5% sodium dodecyl sulfate (SDS) solution (pH 1.9) for 1 min followed by rinsing the probe with PBST.

To measure the detection time, initially, two concentrations of bacterial solutions (10 CFU/mL and 100 CFU/mL) were measured using FC-TGT AuNPs/MoS_2-NPs functionalized non-etched sensor probe and found that sensor is saturated after 5 min and achieves maximum absorbance as shown in Fig. A-7

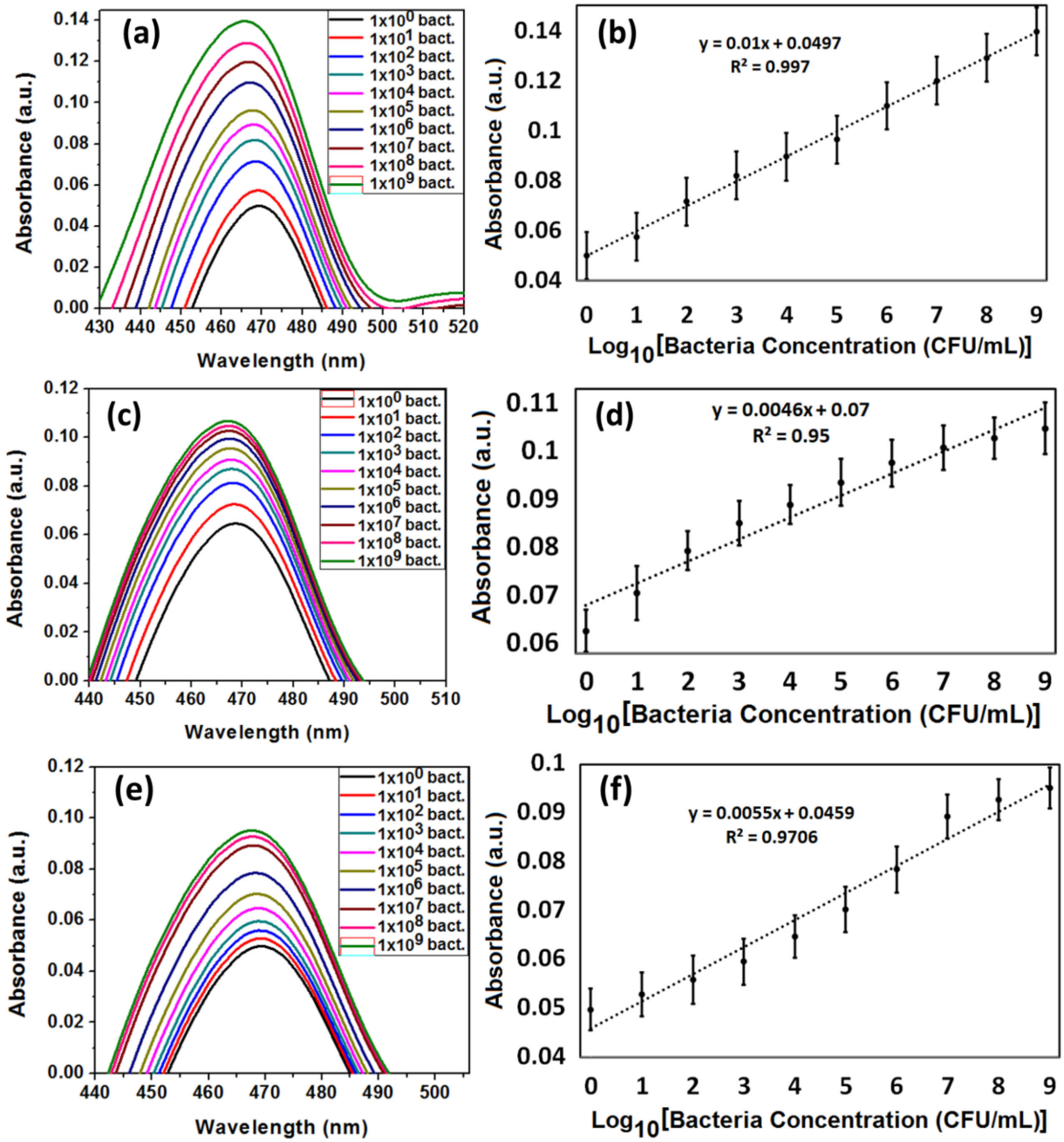

Fig. 4. Bacterial sensing results and linearity plots of (a, b) FC-TGT, (c, d) BPM-TGT, (e, f) NC-TGT using AuNPs/MoS_2-NPs functionalized etched sensor probe.

(Appendix). Thus, detection time of sensor is found as 5 min. Here, absorbance value at t = 0, shows the absorbance in the presence of PBS only, then PBS solution was replaced with the known bacterial concentration.

First, a non-etched fiber structure was used for detection of *S. sonnei* using three Oligonucleotides i.e., FC-TGT, BPM-TGT, and NC-TGT. Fig. A-8a shows the bacterial sensing result of FC-TGT functionalized non-etched sensor probe. The absorbance increases with an increase in *Shigella* concentration (CFU/mL) as the active sites of the probe get blocked and absorb more light. It is well reported that bacterial cells form electrostatic interaction with the metal NPs, helps them to get attached to the NPs coated optical sensor probes [37]. During sensing experiment, the lower concentration to higher concentration of *Shigella* was taken and before detecting the higher concentration, the sensor probe was rinsed with 0.5% SDS solution (pH 1.9) for 1 min to regenerate the sensor probe. Fig. A-8b shows its linearity plot, the linear range of FC-TGT functionalized non-etched sensor probe lies in the range of 1 - 1×10^9 CFU/mL. The sensor shows saturation after 1×10^9 CFU/mL. The limit of detection (LoD) of this sensor probe is 2.30 CFU/mL and its detection time is 5 min. Here, LoD is defined as three times the standard deviation of blank samples multiplied by the inverse of calibration curve slope [1]. Similarly, Fig. A-8c shows the bacterial

sensing result of BPM-TGT functionalized non-etched sensor probe, and Fig. A-8d shows its linearity plot in the range of 1 - 1×10^9 CFU/mL, and its LoD is calculated as 4.89 CFU/mL.

Thereafter, Fig. A-8e shows the bacterial sensing result of NC-TGT functionalized non-etched sensor probe, and Fig. A-8f shows its linearity plot in the range of 1 - 1×10^9 CFU/mL, its LoD is calculated to be 5.59 CFU/mL. Similar experiments were conducted with the etched sensor probes due to their pertinent advantages. In MCF, supermodes are generated due to superposition of isolated linearly polarized (LP) modes in its cores [20]. Due to the core mismatch of SMF-MCF structure, the fundamental modes of SMF excites the supermodes in MCF. Due to etching of MCF structure, these supermodes are enhanced thereby enhancing the sensitivity of the etched system. Here, Fig. A-9a shows the bacterial sensing result of FC-TGT AuNPs-functionalized etched sensor probe with LoD as 1.98 CFU/mL. Due to AuNPs, sensor works on LSPR phenomena but it can be observed from Fig. A-9b is that its accuracy of sensing is too low (0.9235) in comparison to AuNPs/MoS_2-NPs functionalized etched sensor probe (shown in Fig. 4b). Same testing was performed using AuNPs/MoS_2-NPs functionalized etched sensing probe. Fig. 4a shows the bacterial sensing result of FC-TGT AuNPs/MoS_2-NPs functionalized etched sensor probe. It is quite evident from Figs. A-9b and 4b, that there is a significant improvement in sensing accuracy and LoD due to immobilization of MoS_2-NPs over AuNPs. The absorbance changes in the case of etched sensing probe (Fig. 4a) are also high concerning non-etched sensor probe shown in Fig. A-8a. Its linearity plot is observed to be in the range of 1 - 1×10^9 CFU/mL as shown in Fig. 4b. The accuracy also improved and its LoD lowered down to 1.56 CFU/mL in comparison to the non-etched sensor probe.

Similarly, Fig. 4c shows the bacterial sensing result of BPM-TGT functionalized etched sensor probe, and Fig. 4d shows its linearity plot, the LoD, 3.40 CFU/mL that is better than the non-etched BPM-TGT sensor probe. Fig. 4e shows the bacterial sensing result of the NC-TGT functionalized etched sensor probe and Fig. 4f shows its linearity plot in the range of 1 - 1×10^9 CFU/mL, which LoD is 2.85 CFU/mL. These results also show that etched MCF sensing probe is better than the non-etched MCF sensing probe for the detection of *Shigella* bacteria. From the results of Figs. 4 (a-f), it is concluded that a fully-complementary DNA probe exhibits the maximum absorbance variation due to high fluorescence/absorbance in comparison to another DNA probe. It also shows that maximum absorbance change occurs due to specific DNA hybridization, not from the non-specific adsorption. These are the reason behind the lower LoD and higher accuracy in sensing the *Shigella* bacteria.

As per Table II, the FC-TGT is a fully-complementary DNA probe that one responsible for detection of *Shigella*. The other DNA oligonucleotides were used to show the specificity of the sensor probe. The sensor probe was tested using three types of oligonucleotides, FC-TGT, NC-TGT, and BPM-TGT, and found that it shows more selectivity response with FC-TGT. Thus, it also proves that proposed sensor is selective. Overall, as from Table II, FC-TGT etched SMF-MCF sensing probe is better concerning accuracy and LOD.

TABLE II
COMPARISON OF PROPOSED SENSORS

Oligonucleotides	SMF-MCF Fiber	Accuracy	Detection limit (CFU/mL)
FC-TGT	Non-etched	0.9732	2.30
BPM-TGT	Non-etched	0.9568	4.89
NC-TGT	Non-etched	0.9624	5.59
FC-TGT	***Etched***	***0.997***	***1.56***
BPM-TGT	Etched	0.95	3.40
NC-TGT	Etched	0.9706	2.85

TABLE III
COMPARISON WITH EXISTING *SHIGELLA* BIOSENSORS

System	Method	Linear range (CFU/mL)	Detection limit	Detection time	Ref.
n.r.[a]	A*	n.r.[a]	5.8 CFU/vessel in milk	12 min	[39]
n.r.[a]	B*	3×10^3 - 3×10^4	18 CFU/mL in blood	78 min	[38]
n.r.[a]	PCR (Syber green)	1.5×10^6 - 1.5×10^2	1.5×10^3 CFU/g	n.r.[a]	[4]
n.r.[a]	Evanescent wave	1 - 1×10^4	100 CFU/mL	5 min	[1]
Au/MoS_2-NPs	**LSPR**	**1 - 1×10^9**	**1.56 CFU/mL**	**5 min**	**This Work**

[a] not reported, A* - Real-time loop-mediated amplification technique, B* - Voltage controlled signal amplification.

In this work, to nullify the interference of PBS also detected the only PBS buffer using the same fiber, and the absorbance value of only PBS was taken as a blank. Thus, there was no interference of PBS in concentration-dependent absorbance of *Shigella*.

D. Comparison With Existing Shigella Biosensors

Table III shows the comparative study of a few techniques that are reported for *Shigella* detection. The proposed sensor exhibits lower LoD than the other proposed sensors which further suggest the advancement of the sensor reported in the present study. Several methods like loop-mediated amplification technique, PCR, and voltage-controlled signal amplification techniques are available for detection of *Shigella* species [1], [4], [38], [39]. These methods suffer from various drawbacks such as time taking, expensive instrumentation, complex procedure, less specificity, and sensitivity. Due to these limitations, these methods are difficult to be applied in real-time detection of samples. Thus, it is important to develop a fast and more effective method for detection of *Shigella* species. The proposed sensor in the study can detect the bacteria as low as 1.56 CFU/mL, which works well in a real scenario.

IV. CONCLUSION

Present study demonstrated the LSPR based sensitive, repetable, and reusable, specific, fiber optic sensor for detection of *Shigella*. The sensor probe had been fabricated using splicing

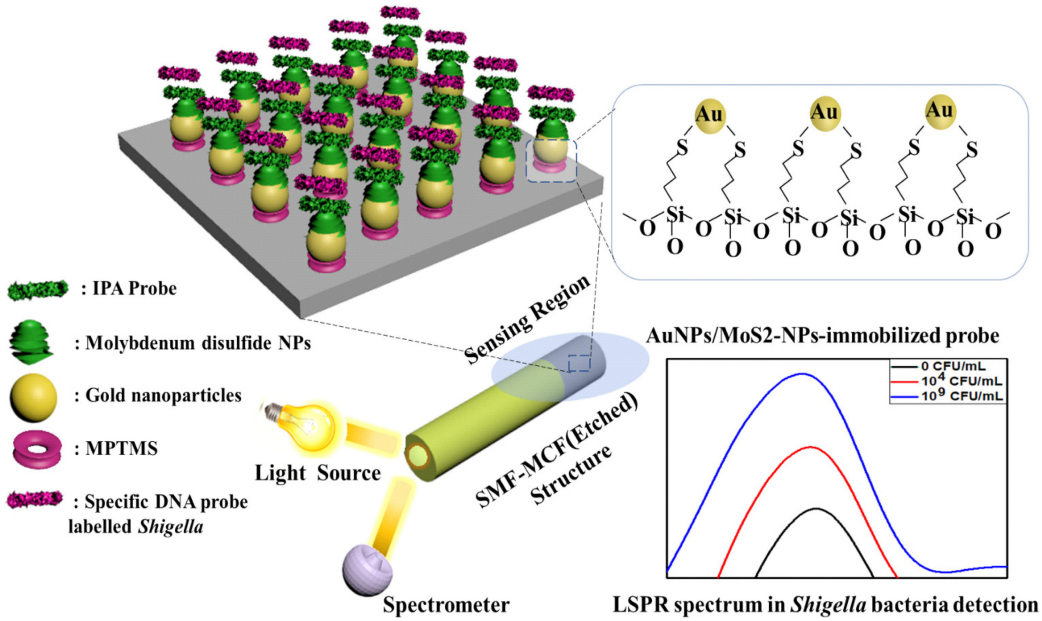

Fig. A-1. Schematic for detection of Shigella bacteria using a proposed sensor probe.

of a short section of MCF with SMF, thereafter coupling of modes was enhanced by etching method. NPs such as AuNPs and MoS_2-NPs have been used to generate localized plasmons and increase sensitivity. To increase the specificity of the sensor, IPA probe has been functionalized over sensor probe, then various DNA oligonucleotides have been used during the detection. FC-TGT oligonucleotides are more responsible for detection of *S. sonnei* than BPM-TGT, and NC-TGT. The sensor works better in the range of 1 - 1×10^9 CFU/mL. The detection limit of etched FC-TGT sensor probe and detection time was 1.56 CFU/mL and 5 min, respectively, which is substantially smaller in comparison to other proposed sensors. Due to low LOD, the proposed sensor is more suitable to diagnose dysentery in the human body. Moreover, this sensor offers other advantages like simplicity, real-time detection, and suitability. The work could focus on the possibility to use the proposed sensor probe to detect other bacteria in the field of aquaculture (*Tenacibaculum Maritimum* and *Vibrio Splendidus*, etc), marine life, etc. The fiber biosensors can be also used for detection of protein, antibodies, toxic gases, metal ions, several serum-based biomolecules.

APPENDIX A

A.I. Experimental Section

A. Synthesis of AuNPs and MoS_2-NPs: Turkevich method was used to synthesize different sizes of AuNPs by varying the concentration of tri-sodium citrate [33]. In proposed work, AuNPs were synthesized and immobilized over the fiber structure to improve the sensitivity of sensor. For this, 15 mL of an aqueous solution of $HAuCl_4$ (150 mL, 100 mM) was boiled at 100 °C. Thereafter, tri-sodium citrate (1.8 mL, 38.8 mM) was added to the boiled solution of $HAuCl_4$. The resultant solution continued to heat and stirred further for 5 min. Then, a red wine color solution appears after 5 min of stirring that shows the preliminary appearance of 10 nm AuNPs.

Molybdenum disulfide nanoparticles (MoS_2 - NPs) were synthesized by ultrasonication of MoS_2 powder in the n-methyl pyrrolidone (NMP) organic solvent [14]. Typically, 30 mg of MoS_2 was added in 10 mL NMP and sonicated for 3 h in the ultrasonic bath machine. Thereafter, homogeneous suspension of MoS_2 was sonicated by a high-power ultra-sonicator for 10 min at room temperature. The output power of 1000 W, with ON and OFF cycle of 9 sec, and 6 sec is used to avoid overheating. Then, the dissolved solution had been centrifuged at 4000 rpm for 1 h at room temperature. The supernatant was collected and stored in the 50 mL glass bottle at room temperature for further use in the experiment.

B. Immobilization of AuNPs and MoS_2-NPs over MCF-SMF sensor probe: The schematic diagram showing step by step immobilization of AuNPs and MoS_2 over the surface of a fiber structure is shown in Fig. 1 [34]. First, a bare fiber structure was cleaned using an ultrasonic machine in acetone for 20 min. Then, fiber structure was kept in Piranha solution (30% H_2O_2 and 70% H_2SO_4) for 30 min to remove the unbounded particles and to produce the OH group over the surface of fiber structure. Afterwards, OH-immobilized fiber was kept in an ethanolic solution of 1% MPTMS for 12 h that helps in immobilizing the AuNPs over the fiber surface.

The unbound MPTMS was removed by rinsing the fiber with ethanol and drying it with nitrogen gas for further process. Thereafter, MPTMS-coated fiber structure was dipped in AuNPs for 48 h. The AuNPs were immobilized over fiber structure through an inexpensive dip-coating technique. The unbounded AuNPs were removed by rinsing the fiber using ethanol and drying it by flowing nitrogen gas. The dip-coating technique was also used for the immobilization of MoS_2-NPs over optical fiber as

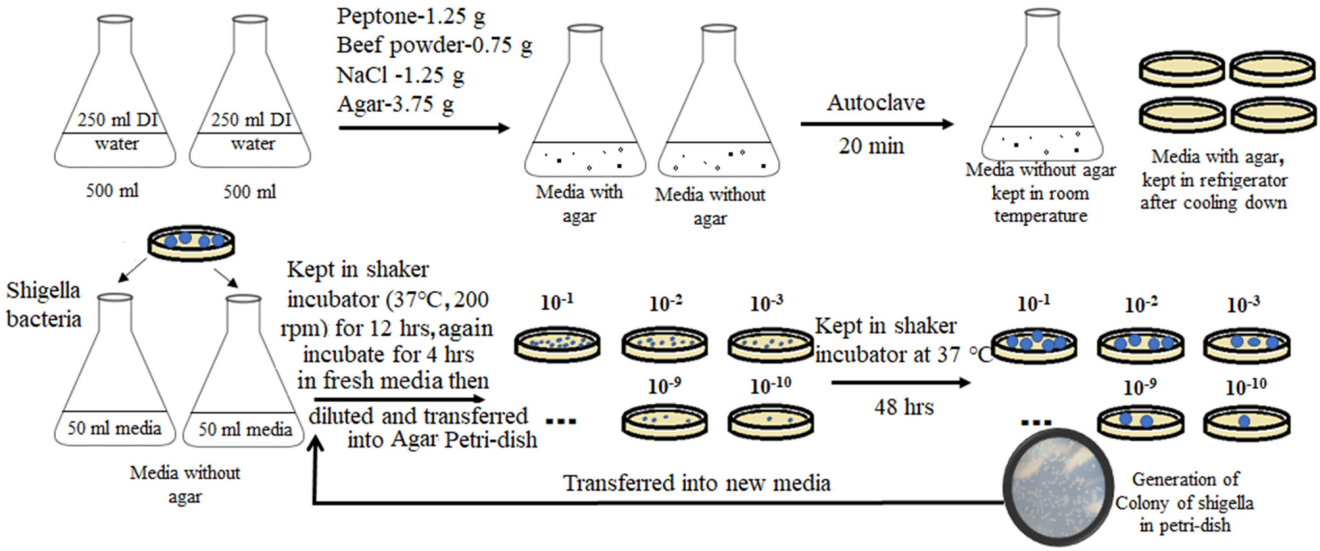

Fig. A-2. Culture steps of *Shigella sonnei* bacteria.

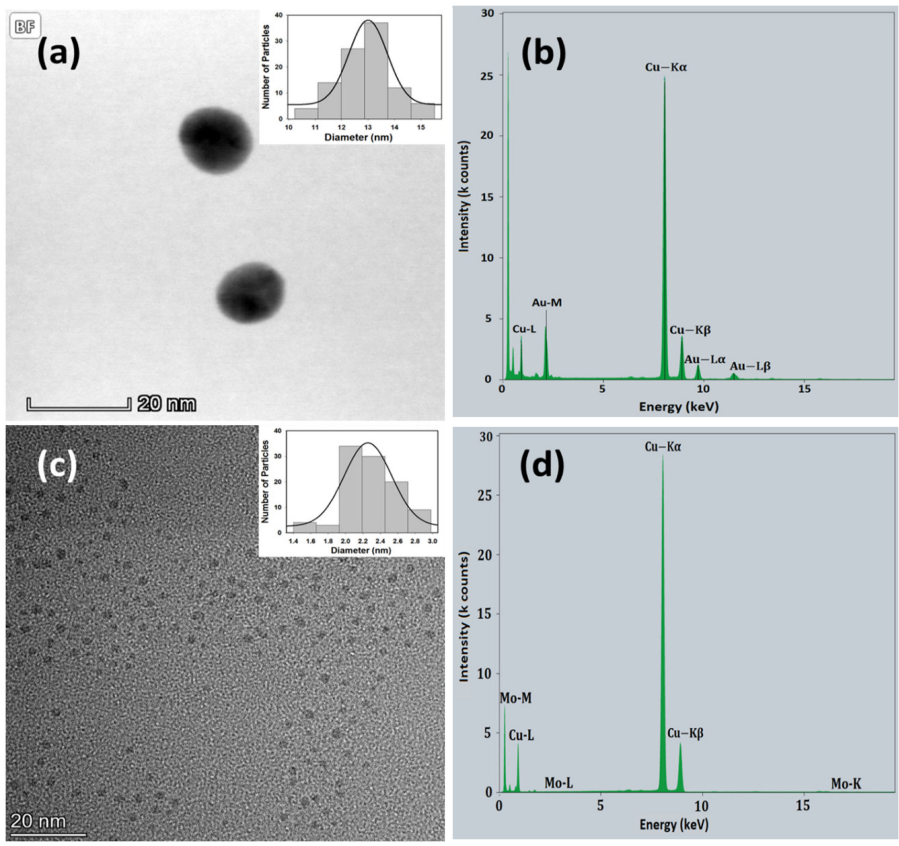

Fig. A-3. High-resolution transmission electron microscopic images of - (a) AuNPs, (c) MoS_2-NPs and energy-dispersive spectroscopic images of - (b) AuNPs, (d) MoS_2-NPs [Inset shows histogram of a diameter of (a) AuNPs, and (b) MoS_2-NPs].

shown in Fig. 1. The AuNPs-coated optical fiber was dipped into 1 mL of MoS_2-NPs solution for 20 sec and dried for 2 min. For uniform coating and proper interface with AuNPs, these steps were carried out several times [14]. Thereafter, immobilized fiber was kept in an oven at 50 °C for 2 h for the proper robustness of MoS_2-NPs.

C. LSPR Measurements: The schematic of the experimental setup is shown in Fig. A-1. It consists of the tungsten-halogen light source (HL-2000, wavelength range: 200–1000 nm, Ocean Optics Inc., USA) and spectrometer (USB2000+, wavelength range: 200–1100 nm, Ocean Optics Inc., USA) as the detector. The IPA-Probe/MoS_2/AuNPs-functionalized SMF-MCF sensor

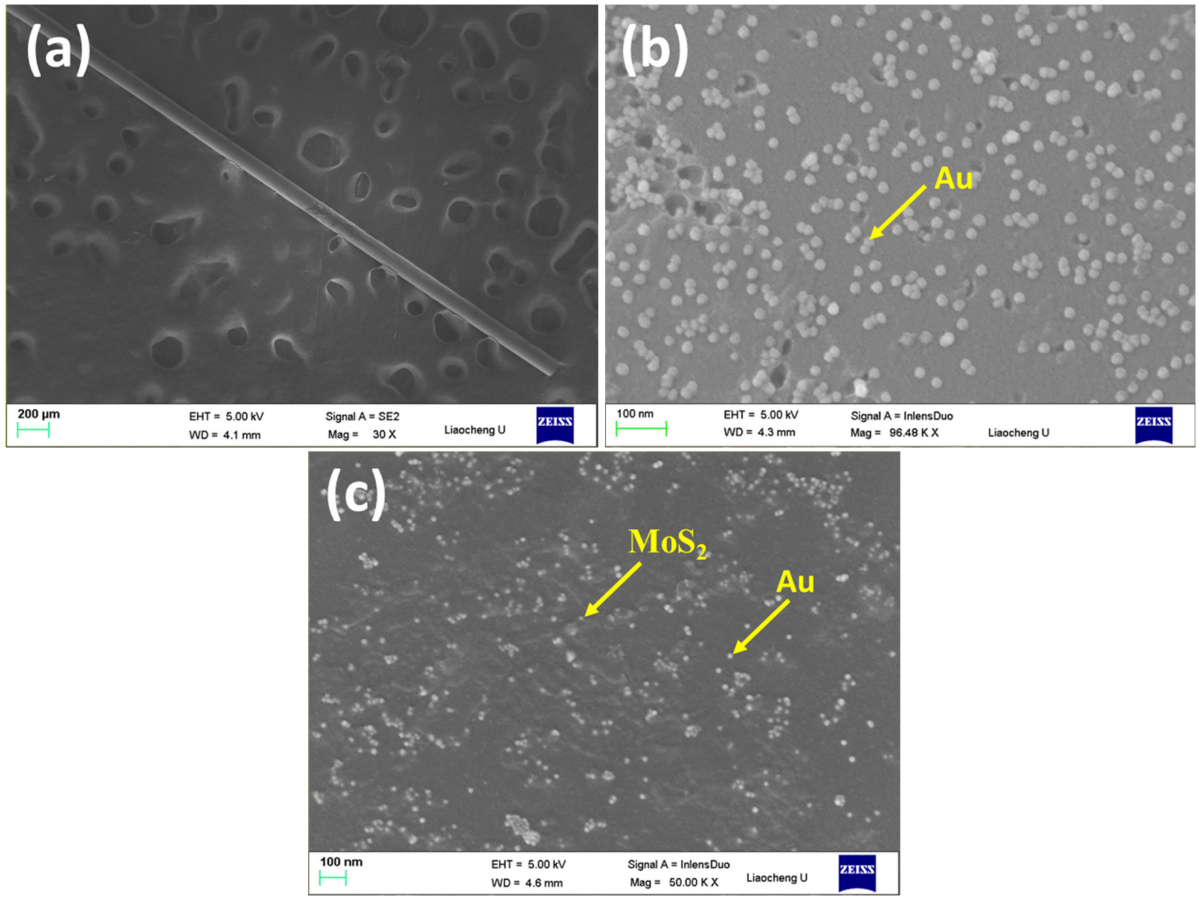

Fig. A-4. (a) SMF-MCF sensor probe, (b) showing the presence of AuNPs, and (c) AuNPs/MoS_2-NPs over sensor probe.

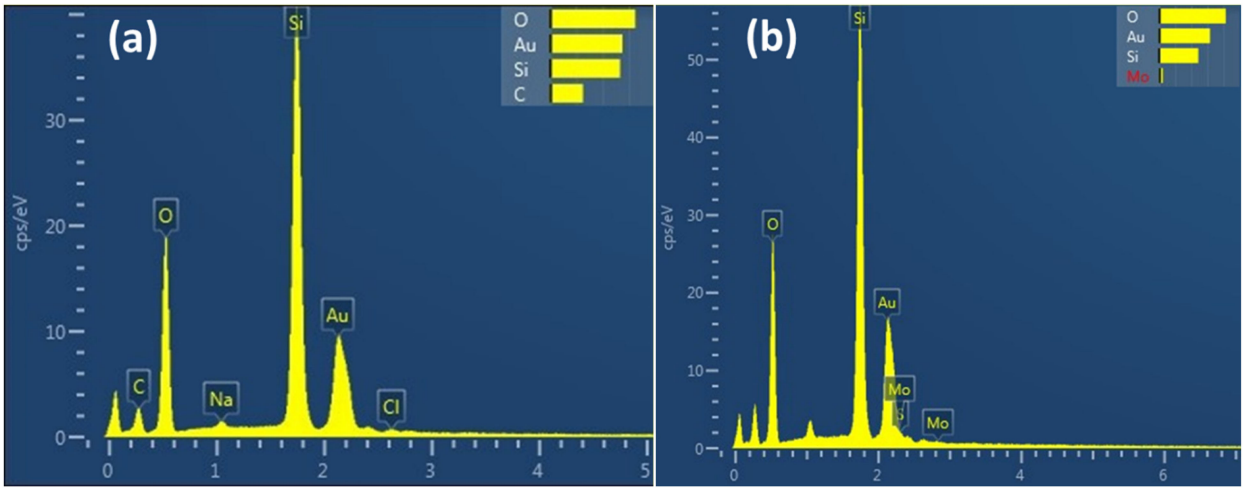

Fig. A-5. SEM-EDS images of (a) AuNPs-immobilized sensor probe, and (b) MoS_2/AuNPs-immobilized sensor probe, showing the presence of Au (a), and Au/Mo (b), respectively.

structure is connected to the bifurcated optical fiber (SPLIT-400-VIS-NIR, Ocean Optics Inc., USA) and inserted into a 1 mL tube consisting of a different bacterial concentration under consideration (CFU/mL). The light source and spectrometer were connected to the first two ports and the sensor probe was connected to the third port of bifurcated optical fiber. First, a blank sample (only PBS) was measured as a reference signal then a different concentration of *Shigella* bacteria prepared in PBS solution was injected around the sensing probe and corresponding LSPR spectra were recorded. Then, sensing probe was rinsed using a 0.5% SDS solution (pH 1.9) for 1 min followed by rinsing the probe with PBST to remove the previous *Shigella*

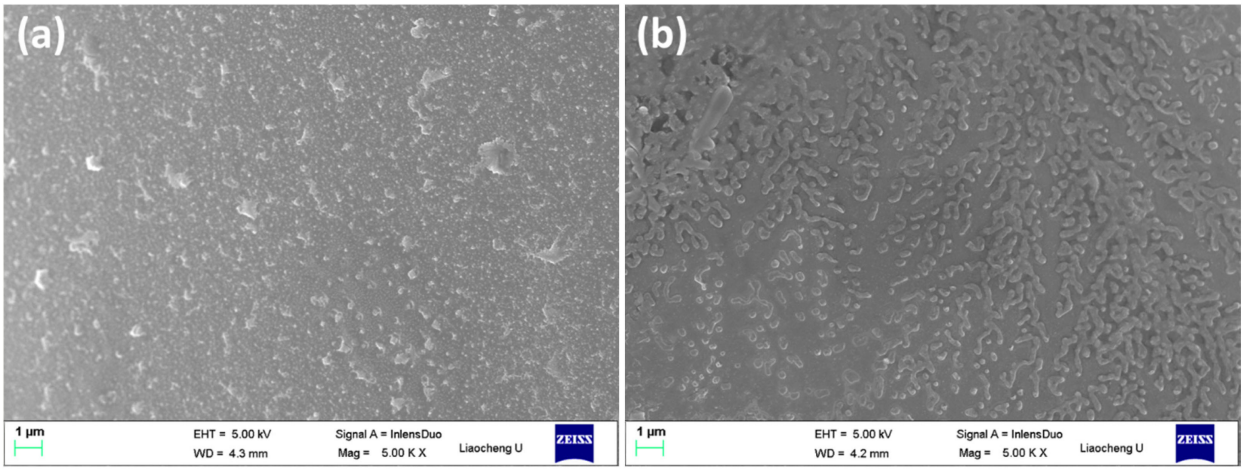

Fig. A-6. SEM images of sensor probe (a) before, and (b) after detection.

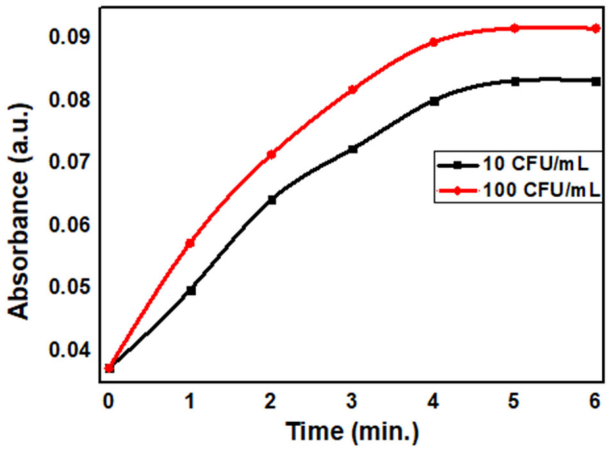

Fig. A-7. Detection of (10, and 100 CFU/mL) *S. sonnei* using FC-TGT AuNPs/MoS_2-NPs functionalized non-etched sensor probe for 6 min.

bacteria and dried after each measurement. The LSPR spectra were recorded through Ocean View software of spectrometer connected to the computer. The proposed sensor works on the principle of LSPR phenomena that states that absorbance value changes due to the variation in the RI surrounding the sensor probe [35].

D. Culture of Shigella sonnei Bacteria: S. sonnei were cultured in the medium containing 1.25 g of peptone, 0.75 g of beef powder, 1.25 g of NaCl in 250 mL DI water with or without 3.75 g of agar. The bacterial concentration was determined using a conventional surface plate count method as shown in Fig. A-2. *S. sonnei* was added in the flask containing media using tip probe and kept in a shaker incubator at 37 °C, 200 rpm, overnight. The bacteria grown in the media overnight were diluted to different concentrations. 50 µL of diluted bacterial culture was added into petri-dish and kept in an incubator at 37 °C for 48 hours in aerobic conditions for further growth of bacterial colonies. Thereafter, bacterial colonies were counted manually at different concentrations, and CFU/mL was calculated as shown in Fig. A-13. For sensing, the bacterial solution was serially diluted to the desired concentration using bacterial media. Then, the specific sequences of 200 µL of aptamer/oligonucleotide (Cy-5 labelled sequences) were allowed to bind with the 1 mL of *Shigella Sonnei* in the presence of media for 5 min. Thereafter, solution of each concentration was centrifuged at 4000 rpm for 5 min to obtain the pellet of bacterial cells and to remove the interference of bacterial media. Further, the pellet was diluted in 1 mL of phosphate buffer saline (1X PBS) buffer solution for measurement.

A.II. Results and Discussion

To confirm the immobilization of AuNPs and AuNPs/MoS_2 over sensor structure, SEM-EDS of nanoparticles coated sensor structure was also performed. Fig. A-5 shows SEM-EDS images of (a) AuNPs-immobilized sensor probe, and (b) MoS_2/AuNPs-immobilized sensor probe, showing the presence of Au (a), and Au/Mo (b), respectively. Now, these images depict that Au is present in Fig. A-4b (AuNPs-immobilized probe) and Au/Mo are present in Fig. A-4c (AuNPs/MoS_2-immobilized probe). In these figures, other materials are found due to composition of fiber structure (Silica, SiO_2) and reagent used in synthesis of AuNPs and MoS_2.

E. Performance Study: Repeatability and Reproducibility Test: To test the repeatability, 10^6 CFU/mL of *Shigella* bacterial solution was measured using FC-TGT AuNPs/MoS_2-NPs functionalized etched sensor probe then sensor probe was regenerated using 0.5% SDS solution (pH 1.9) for 1 min followed by rinsing the probe with PBST. Thereafter, same concentration of new solution was detected and found there is negligible change in absorbance as shown in Fig. A-10a. This result shows that repeatability of sensor probe is better.

Similarly, to test the reproducibility, three similar sensors were fabricated with the optimized parameter and protocol as discussed in paper, and tested the 10^4 CFU/mL *Shigella* bacterial solution. Fig. A-10b shows the bacterial sensing results of three sensors based on FC-TGT AuNPs/MoS_2-NPs functionalized

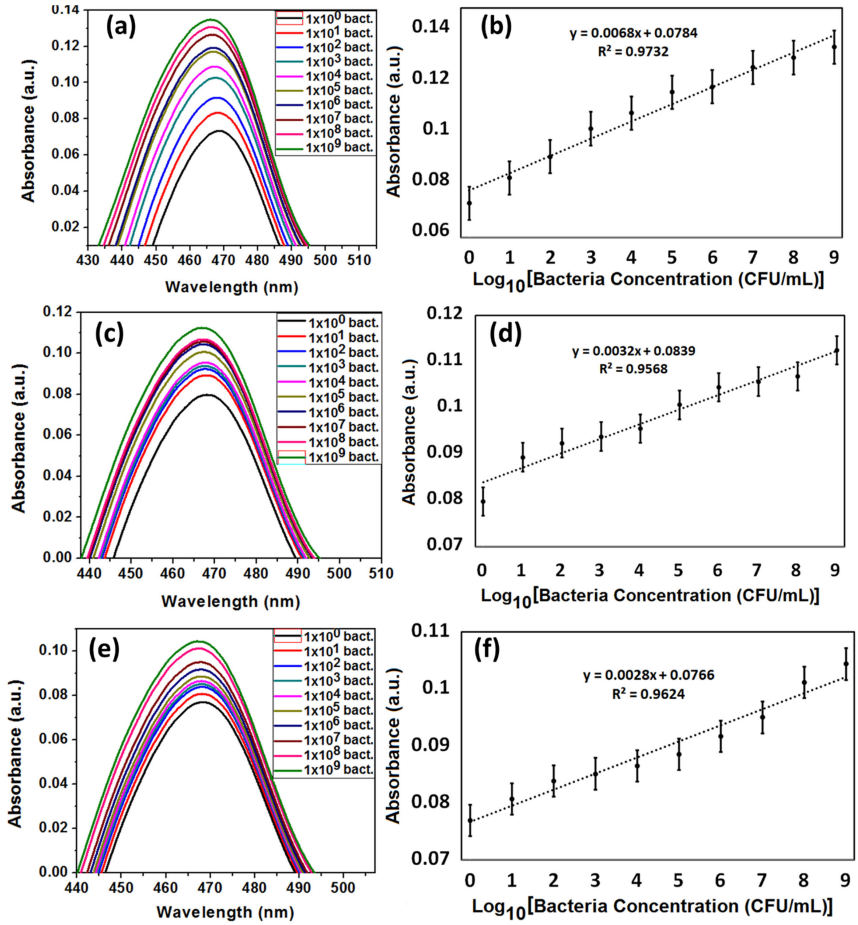

Fig. A-8. Bacterial sensing results and linearity plots of (a, b) FC-TGT, (c, d) BPM-TGT, (e, f) NC-TGT using AuNPs/MoS_2-NPs functionalized nonetched sensor probe.

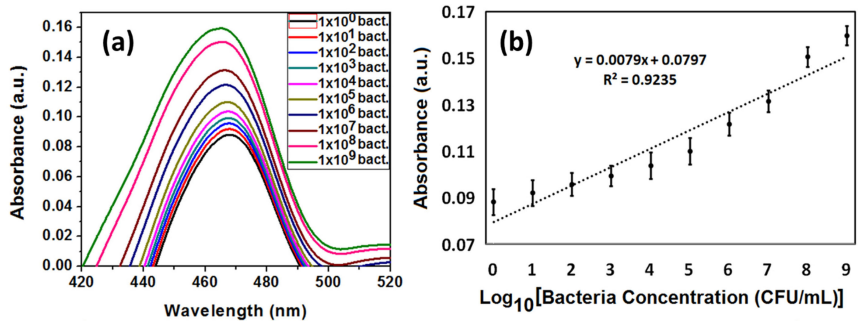

Fig. A-9. (a) Bacterial sensing results, and (b) linearity plots of FC-TGT AuNPs- functionalized etched sensor probe.

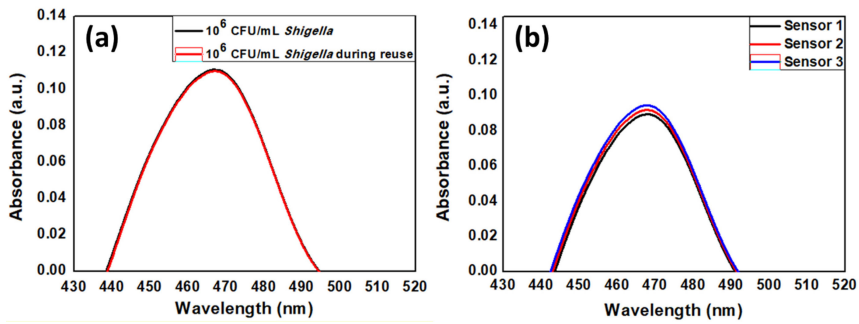

Fig. A-10. (a) Repeatability, (b) and reproducibility test using FC-TGT AuNPs/MoS_2-NPs functionalized etched sensor probe.

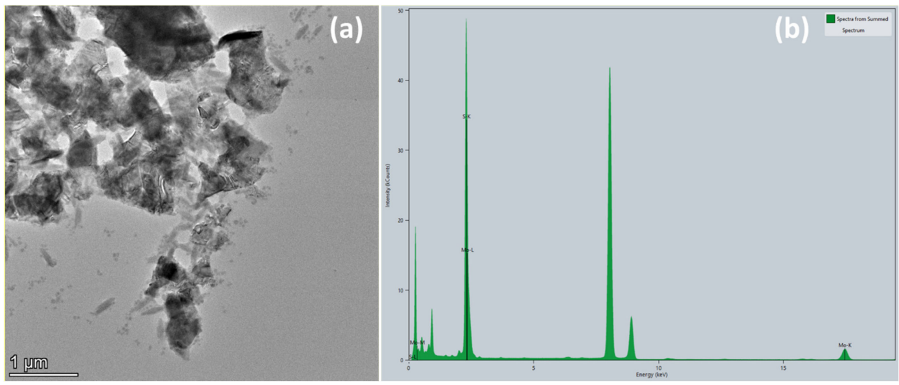

Fig. A-11. (a) HR-TEM image of synthesized MoS_2 – nanosheet, and (b) EDS image confirms that the synthesized nanosheet is molybdenum (Mo).

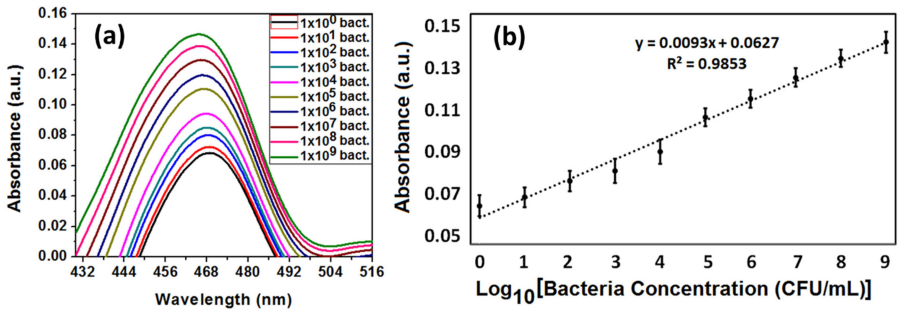

Fig. A-12. (a) Bacterial sensing results, and (b) linearity plots of FC-TGT AuNPs/ MoS_2-Sheet functionalized etched sensor probe.

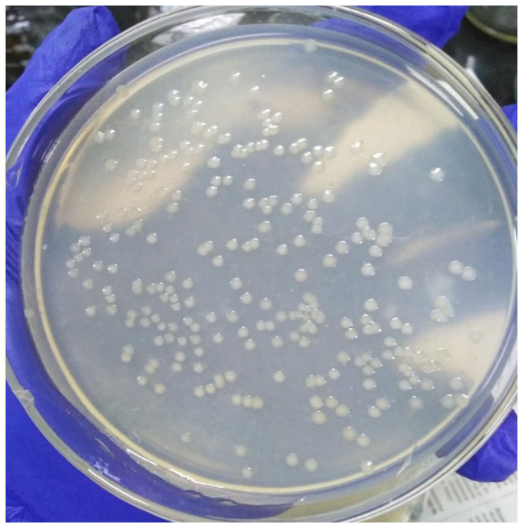

Fig. A-13. *Shigella sonnei* colony in the flask.

etched sensor probe. There is an insignificant variation in absorbance of sensing result of three sensors and standard error is too low, it means reproducibility of sensor is also good.

Effect of Temperature: A well-defined incubation conditions and nutrition's were required for *Shigella sonnei* bacteria. There was aerobic condition and 37 °C culture temperature for growth and survival of this type of bacteria. Thus, an incubator was used to keep pre-defined temperature. As, main objective in this work was to detect the live bacterial cells, thus 1 ml tube of bacterial solutions were kept in a dry bath at 37 °C during the measurement. *Shigella sonnei* bacteria cannot survive at different incubation conditions and give the proper results of measurement.

MoS_2-Sheet: Further, to check the performance of molybdenum disulfide (MoS_2) nanosheet and nanoparticles, an experiment was carried out with the functionalization of MoS_2-nanosheet at the place of nanoparticles. For this purpose, first MoS_2–nanosheet was synthesized as per protocol discussed by Kaushik *et al.* [14]. Here, Fig. A-11a shows the HR-TEM image of synthesized MoS_2 – nanosheet, and Fig. A-11b confirms that the synthesized nanosheet is molybdenum (Mo). Thereafter, same protocol as discussed earlier was used for functionalization of MoS_2 – nanosheet over optical fiber structure.

Here, Fig. A-12a shows the bacterial sensing result of FC-TGT AuNPs/MoS_2-sheet functionalized etched sensor probe. As per linearity plot shown in Fig. A-12b, its accuracy is 0.9853, and LoD is obtained as 1.68 CFU/mL.

Fig. 4a shows the bacterial sensing result of FC-TGT AuNPs/MoS_2-nanoparticles functionalized etched sensor probe and its LoD and accuracy are 1.56 CFU/mL and 0.997 obtained from linearity plot shown in Fig. 4b. Thus, based on the experimental results it can be concluded that sensing performance of MoS_2-nanoparticles is better than MoS_2-nanosheet. It is due to a higher surface area of smaller size (approx. 2.2 nm) of MoS_2-NPs.

REFERENCES

[1] R. Xiao, Z. Rong, F. Long, and Q. Liu, "Portable evanescent wave fiber biosensor for highly sensitive detection of shigella," *Spectrochimica Acta Part A: Mol. Biomol. Spectrosc.*, vol. 132, pp. 1–5, Nov. 2014.

[2] G. G. Huang, C. J. Lee, B. C. Tsai, J. Yang, M. Sathiyendiran, and K. L. Lu, "Gondola-shaped tetra-rhenium metallacycles modified evanescent wave infrared chemical sensors for selective determination of volatile organic compounds," *Talanta*, vol. 85, pp. 63–69, Jul. 2011.

[3] X. Mao, L. Yang, X. L. Su, and Y. Li, "A nanoparticle amplification based quartz crystal microbalance DNA sensor for detection of Escherichia Coli O157:H7," *Biosens. Bioelectron.*, vol. 21, pp. 1178–1185, Jan. 2006.

[4] W. Mokhtari, S. Nsaibia, A. Gharbi, and M. Aouni, "Real-time PCR using SYBR green for the detection of Shigella spp. in food and stool samples," *Mol. Cell Probes*, vol. 27, pp. 53–59, Feb. 2013.

[5] W. Wu *et al.*, "An aptamer-based biosensor for colorimetric detection of Escherichia Coli O157:H7," *PLoS One*, vol. 7, 2012, Paper e48999.

[6] R. Srinivasan, S. Umesh, S. Murali, S. Asokan, and S. Siva Gorthi, "Bare fiber bragg grating immunosensor for real-time detection of Escherichia Coli bacteria," *J. Biophoton.*, vol. 10, pp. 224–230, Feb 2017.

[7] N. H. Zainuddin, H. Y. Chee, M. Z. Ahmad, M. A. Mahdi, M. H. A. Bakar, and M. H. Yaacob, "Sensitive leptospira DNA detection using tapered optical fiber sensor," *J. Biophoton.*, vol. 11, Aug. 2018, Paper e201700363.

[8] P. K. Maharana, S. Bharadwaj, and R. Jha, "Electric field enhancement in surface plasmon resonance bimetallic configuration based on chalcogenide prism," *J. Appl. Phys.*, vol. 114, 2013, Art. no. 014304.

[9] P. K. Maharana, T. Srivastava, and R. Jha, "Low index dielectric mediated surface plasmon resonance sensor based on graphene for near infrared measurements," *J. Phys. D: Appl. Phys.*, vol. 47, 2014, Art. no. 385102.

[10] J. K. Nayak, P. Parhi, and R. Jha, "Experimental and theoretical studies on localized surface plasmon resonance based fiber optic sensor using graphene oxide coated silver nanoparticles," *J. Phys. D Appl. Phys.*, vol. 49, Jul. 01, 2016, Art. no. 285101.

[11] M. Ben Haddada *et al.*, "Gold nanoparticle-based localized surface plasmon immunosensor for staphylococcal enterotoxin a (SEA) detection," *Anal Bioanal. Chem.*, vol. 409, pp. 6227–6234, Oct 2017.

[12] H. Jans and Q. Huo, "Gold nanoparticle-enabled biological and chemical detection and analysis," *Chem. Soc. Rev.*, vol. 41, pp. 2849–2866, Apr. 2012.

[13] N. Agrawal *et al.*, "Detection of L-Cysteine using silver nanoparticles and graphene oxide immobilized tapered SMS optical fiber structure," *IEEE Sensors J.*, vol. 20, pp. 11372–11379, Oct.,1 2020.

[14] S. Kaushik, U. K. Tiwari, S. S. Pal, and R. K. Sinha, "Rapid detection of escherichia coli using fiber optic surface plasmon resonance immunosensor based on biofunctionalized molybdenum disulfide (MoS_2) nanosheets," *Biosens. Bioelectron.*, vol. 126, pp. 501–509, 2019.

[15] S. Zeng *et al.*, "Graphene–MoS_2 hybrid nanostructures enhanced surface plasmon resonance biosensors," *Sensors Actuators B: Chem.*, vol. 207, pp. 801–810, 2015.

[16] J. K. Nayak, P. K. Maharana, and R. Jha, "Dielectric over-layer assisted graphene, its oxide and MoS_2-based fibre optic sensor with high field enhancement," *J. Phys. D: Appl. Phys.*, vol. 50, 2017, Art. no. 405112.

[17] P. Halkare, N. Punjabi, J. Wangchuk, K. Kondabagil, and S. Mukherji, "LSPR based fiber optic sensor for detection of e. coli using bacteriophage t4," in *Proc. Workshop Recent Adv. Photon. (WRAP)*, 2015, pp. 1–4.

[18] Y. Chunxia, D. Hui, D. Wei, and X. Chaowei, "Weakly-coupled multicore optical fiber taper-based high-temperature sensor," *Sensors Actuators A: Phys.*, vol. 280, pp. 139–144, 2018.

[19] M.-J. Li and T. Hayashi, "Chapter 1 - Advances in low-loss, large-area, and multicore fibers," in *Opt. Fiber Telecommun. VII*, A. E. Willner, Ed.. Cambridge, MA, USA: Academic, 2020, pp. 3–50.

[20] C. Zhang, T. Ning, J. Li, L. Pei, C. Li, and H. Lin, "Refractive index sensor based on tapered multicore fiber," *Opt. Fiber Technol.*, vol. 33, pp. 71–76, 2017.

[21] Z. A. A. Al-Mashhadani and I. Navruz, "Highly sensitive measurement of surrounding refractive index using tapered trench–assisted multicore fiber," *Opt. Fiber Technol.*, vol. 48, pp. 76–83, 2019.

[22] R. Singh *et al.*, "Etched multicore fiber sensor using copper oxide and gold nanoparticles decorated graphene oxide structure for cancer cells detection," *Biosens. Bioelectron.*, vol. 168, 2020, Art. no. 112557.

[23] D. Barrera, J. Madrigal, S. Delepine-Lesoille, and S. Sales, "Multicore optical fiber shape sensors suitable for use under Gamma radiation," *Opt. Express*, vol. 27, pp. 29026–29033, 2019.

[24] J. Villatoro, E. Antonio-Lopez, A. Schülzgen, and R. Amezcua-Correa, "Miniature multicore optical fiber vibration sensor," *Opt. Lett.*, vol. 42, pp. 2022–2025, 2017.

[25] Z. Zhao *et al.*, "Robust in-fiber spatial interferometer using multicore fiber for vibration detection," *Opt Express*, vol. 26, pp. 29629–29637, Nov. 2018.

[26] I. Floris, J. Madrigal, S. Sales, P. A. Calderón, and J. M. Adam, "Twisting measurement and compensation of optical shape sensor based on spun multicore fiber," *Mech. Syst. Signal Process.*, vol. 140, 2020, Art. no. 106700.

[27] L. Duan *et al.*, "Heterogeneous all-solid multicore fiber based multipath michelson interferometer for high temperature sensing," *Opt. Express*, vol. 24, pp. 20210–20218, 2016.

[28] X. Zhan *et al.*, "Few-mode multicore fiber enabled integrated mach-zehnder interferometers for temperature and strain discrimination," *Opt. Express*, vol. 26, pp. 15332–15342, 2018.

[29] J. A. Vallés and D. Benedicto, "Optimized active multicore fiber bending sensor," *Opt. Mater.*, vol. 87, pp. 53–57, 2019.

[30] J. Villatoro, A. Van Newkirk, E. Antonio-Lopez, J. Zubia, A. Schülzgen, and R. Amezcua-Correa, "Ultrasensitive vector bending sensor based on multicore optical fiber," *Opt. Lett.*, vol. 41, pp. 832–835, 2016.

[31] Y. Amma, K. Takenaga, S. Matsuo, and K. Aikawa, "Fusion splice techniques for multicore fibers," *Opt. Fiber Technol.*, vol. 35, pp. 72–79, 2017.

[32] S. Kumar, R. Singh, Q. Yang, S. Cheng, B. Zhang, and B. K. Kaushik, "Highly sensitive, selective and portable sensor probe using germanium-doped photosensitive optical fiber for ascorbic acid detection," *IEEE Sensors J.*, early access, Feb. 12, 2020, doi:10.1109/JSEN.2020.2973579.

[33] J. Turkevich, P. C. Stevenson, and J. Hillier, "A study of the nucleation and growth processes in the synthesis of colloidal gold," *Discuss. Faraday Soc.*, vol. 11, pp. 55–75, 1951.

[34] N. Agrawal, B. Zhang, C. Saha, C. Kumar, X. Pu, and S. Kumar, "Ultra-Sensitive cholesterol sensor using gold and zinc-oxide nanoparticles immobilized core mismatch MPM/SPS probe," *J. Lightw. Technol.*, vol. 38, pp. 2523–2529, 2020.

[35] P. Sharma, V. Semwal, and B. D. Gupta, "A highly selective LSPR biosensor for the detection of taurine realized on optical fiber substrate and gold nanoparticles," *Opt. Fiber Technol.*, vol. 52, 2019, Art. no. 101962.

[36] J. Feng, Q. Shen, J. Wu, Z. Dai, and Y. Wang, "Naked-eyes detection of Shigella flexneri in food samples based on a novel gold nanoparticle-based colorimetric aptasensor," *Food Control*, vol. 98, pp. 333–341, 2019.

[37] R. Singh and S. Singh, "Uptake and toxicity of different nanoparticles towards a tough bacterium: Deinococcus radiodurans, " *Adv. Mater. Lett.*, vol. 9, pp. 531–537, 2018.

[38] J. Luo, J. Wang, A. Mathew, and S.-T. Yau, "Ultrasensitive detection of Shigella species in blood and stool," *Anal. Chem.*, vol. 88, pp. 2010–2014, 2016.

[39] Y. Wang *et al.*, "Rapid and sensitive detection of shigella spp. and salmonella spp. by multiple endonuclease restriction real-time loop-mediated isothermal amplification technique," *Front Microbiol*, vol. 6, 2015, Art. no. 1400.